Transient Inclusion Evolution During Modification of Alumina Inclusions by Calcium in Liquid Steel: Part I. Background, Experimental Techniques and Analysis Methods

NEERAV VERMA, PETRUS C. PISTORIUS, RICHARD J. FRUEHAN, MICHAEL POTTER, MINNA LIND, and SCOTT STORY

In aluminum-killed steels, modification of solid alumina inclusions is often carried out by calcium treatment, converting the alumina to liquid calcium aluminates. When calcium treatment is performed, calcium can either react with sulfur in the melt or with solid alumina. Calcium sulfide inclusions are solid at steel casting temperatures and thus would be detrimental to castability if they remained in the steel after calcium treatment. The aim was to study the transient evolution of inclusions after calcium treatment, testing the hypothesis that calcium sulfide may form as an intermediate reaction product, which can subsequently react with alumina to form modified calcium aluminates. The first part gives the project background and describes the experimental and quantification techniques adopted, including the effect of sampler size in laboratory melts. Results of the formation of intermediate calcium reaction products in laboratory and industrial heats are presented in the second part.

DOI: 10.1007/s11663-011-9516-3

I. INTRODUCTION

THE production of clean steel involves the control, elimination, or modification of nonmetallic inclusions.[1] In Al-killed steels, alumina (Al_2O_3) is the main inclusion type. In some cases, these inclusions also can contain some MgO,[2,3] but the work presented here focuses on alumina inclusions and their modification. Calcium treatment, by powder injection or wire feeding, is commonly used to modify solid alumina inclusions to form calcium aluminates, which can be fully or partially liquid, depending on the CaO content.[4] Liquid inclusions improve steel castability. The following reaction sequence [1] summarizes the conventional view[5,6] of the reactions after calcium injection, which include melting, vaporization, and dissolution (in liquid steel) of the calcium as well as a reaction with alumina, dissolved oxygen, and dissolved sulfur:

$$\begin{aligned} &Ca(s) \rightarrow Ca(l) \rightarrow Ca(g) \rightarrow [Ca] \\ &[Ca] + [O] \rightarrow CaO \\ &[Ca] + [S] \rightarrow CaS \\ &[Ca] + (x + 1/3)\ Al_2O_3 \rightarrow CaO \cdot xAl_2O_3 + 2/3\,[Al] \end{aligned} \qquad [1]$$

The importance and role of CaS formation are not clear from previous works. CaS is not stable in contact with unmodified or $CaAl_2O_4$-saturated modified inclusions in aluminum-killed steel if the dissolved sulfur content is less than approximately 300 ppm at 1873 K (1600 °C) (Figure 1). In Figure 1, CaS is an equilibrium-stable phase for steel compositions above the line. Based on these facts, it can be concluded that the extent of CaS formation at typical sulfur levels in steel is negligible.[6] However, CaS was reported to form as a transient phase[9–11] immediately upon calcium injection,[3] or perhaps only after calcium aluminates have formed.[11] The subsequent reaction mechanism of CaS is similarly unclear; suggestions include the evaporation of calcium[10] or an unspecified reaction leading to equilibration (*i.e.*, consumption of CaS).[11] Our preliminary work supported a direct role of CaS in the modification of alumina for 3-kg laboratory steel melts containing 45 ppm S and 0.04 to 0.05 pct Al. The transient CaS inclusions in contact with unmodified alumina were observed in steel samples taken immediately after calcium addition, whereas steel samples that were taken later on contained partially modified (calcium aluminate) inclusions with much lower sulfur contents.[3] It is hence proposed that the CaS can react with the alumina to yield modified inclusions according to reaction [2] (dissolved calcium may be a reaction intermediate, but because of the uncertainty regarding the concentration of dissolved calcium in liquid steel,[12,13] this is not explicitly included in the reaction). The reaction is expressed as follows:

$$3CaS + Al_2O_3 \rightarrow 3(CaO) + 2[Al] + 3[S] \qquad [2]$$

Through the formation of CaS as a transient phase, sulfur in the steel may assist in modification by

NEERAV VERMA, Ph.D. Candidate, and PETRUS C. PISTORIUS and RICHARD J. FRUEHAN, Professors, are with the Center for Iron and Steelmaking Research, Department of Materials Science and Engineering, Carnegie Mellon University, Pittsburgh, PA 15213. Contact e-mail: pcp@andrew.cmu.edu MICHAEL POTTER, Senior Scientist, is with the RJ Lee Group, Monroeville, PA 15146. MINNA LIND, formerly Visiting Researcher at Carnegie Mellon University, is now with Aalto University, FI-00076 Aalto, Finland. SCOTT STORY, Research Consultant, is with the United States Steel Corporation Research and Technology Center, Munhall, PA 15120.

Manuscript submitted February 24, 2011.
Article published online April 12, 2011.

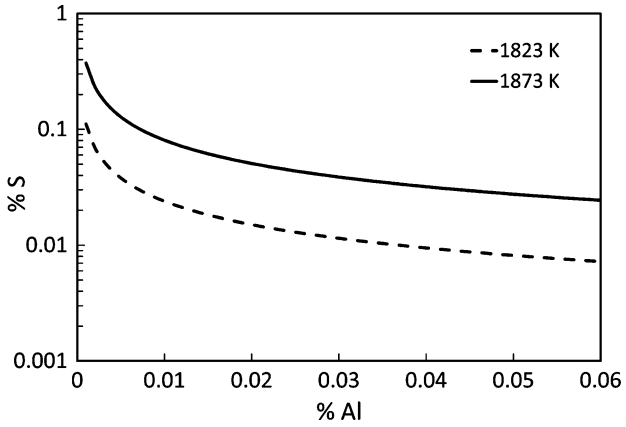

Fig. 1—Calculated Al-S equilibrium curves for $a_{CaS} = 1$ (solid reference state) in contact with liquid CaO-Al_2O_3 (at $CaAl_2O_4$ saturation) in steel, for 1823 K and 1873 K (1550 °C and 1600 °C). Reaction equilibrium constant and CaO and Al_2O_3 activities taken from FactSage[7]; free energy of solution of sulfur and aluminum in steel taken from Sigworth and Elliott.[8]

capturing calcium, which can subsequently react with alumina. The possible extent of calcium capture would depend on the sulfur content of the steel. For a typical total oxygen content of 20 ppm in the steel (mostly in the form of alumina [Al_2O_3]), the minimum amount of calcium required to transform alumina inclusions into liquid calcium aluminates would be about 13 ppm. This corresponds to a minimum of 10 ppm S required to capture the injected calcium if S were responsible for capturing all of the calcium. A different modification mechanism is hence expected in steel containing less than approximately 10 ppm S, which was tested experimentally.

The work presented here aims to verify the formation and role of transient calcium sulfide by analyzing the evolution of inclusion size, shape, and composition after calcium treatment. Laboratory experiments and industrial heats were considered using aluminum-killed steel with sulfur contents between 7 ppm and 100 ppm.

When examining inclusions in samples of calcium-treated steel, care should be taken to distinguish ways in which calcium sulfide can form. The three known origins of CaS coexisting with oxide inclusions are as follows:

(a) Stable CaS, formed by Ca treatment of high-sulfur steels, or over-modification (adding more calcium than needed to modified alumina inclusions)[6,14]
(b) CaS ring formation around a modified calcium aluminate, formed during solidification as a result of sulfur enrichment in the residual liquid metal around a modified inclusion[15]
(c) Transient CaS formation (often in contact with unmodified inclusions).[3,9–11]

Inclusions containing CaS of types (b) and (c) were observed in this work. These inclusions were distinguished readily because no ring-shaped deposit of CaS was found shortly after calcium treatment; transient CaS was generally present as discrete particles, often in contact with alumina, but never as a ring around alumina.

II. METHODOLOGY

Laboratory-scale melts and industrial heats were studied, using samples taken after aluminum deoxidation and at various times after calcium treatment. Scanning electron microscopy with energy dispersive spectrometry (SEM/EDS) of polished steel sample cross sections were used to characterize inclusion shape, size, and composition. Both automated and manual microanalyses were used. Industrial samples were also analyzed.

A. *Materials*

Laboratory melts were prepared with high-purity electrolytic iron (12-mm diameter pieces), using aluminum shot (99.999 pct, 5-mm diameter) for deoxidation. Calcium disilicide ($CaSi_2$) powder was used for calcium treatment. A high-purity (99.9 pct) porous MgO crucible (outer diameter 86 mm, inner diameter 71 mm, and height 160 mm) was employed to melt iron. Various sampling tubes were used, and the effect of the sampling tube size was also studied (comparing larger-diameter, gravity-fed quartz tubes with smaller-diameter, vacuum samplers). To test the effect of sulfur in the melt on the extent of modification of oxide inclusions, FeS (iron II sulfide—99.99 pct purity) was used to adjust the sulfur content of the melt (FeS was added with the iron before deoxidation).

B. *Experimental Setup*

Figure 2 shows a schematic diagram of the experimental setup for laboratory melts. A 15-kW vacuum induction furnace was employed for melting, additions and sampling the steel.[16] This furnace was used to reduce reoxidation of the melt by the atmosphere, which would have altered the inclusion and melt chemistries. The vacuum system connected to the induction furnace (mechanical pump and diffusion pump) could evacuate the chamber to about 1 Pa prior to backfilling with argon. A dual-wavelength pyrometer measured the melt temperature through a top window. Two manipulators with sampling tools (Figure 2) were used to make additions and take samples. The manipulators allowed for rotation and vertical movement of the sampling tools without exposing the melt to atmosphere, thus avoiding reoxidation of the steel.

C. *Experimental Procedure*

Figure 3 shows a flowchart of the experimental procedure. The chamber was evacuated with the mechanical and diffusion pumps and then backfilled with high-purity argon to atmospheric pressure. A total of 3 kg of electrolytic iron chips was melted in an MgO crucible, first melting about 0.8 kg of electrolytic iron, before adding the remaining 2.2 kg in batches when the initial iron had melted. This stepwise addition was used to avoid bridging the electrolytic iron chips in the crucible. The oxygen content of the liquid iron (before Al deoxidation) was measured to be about 400 ppm.

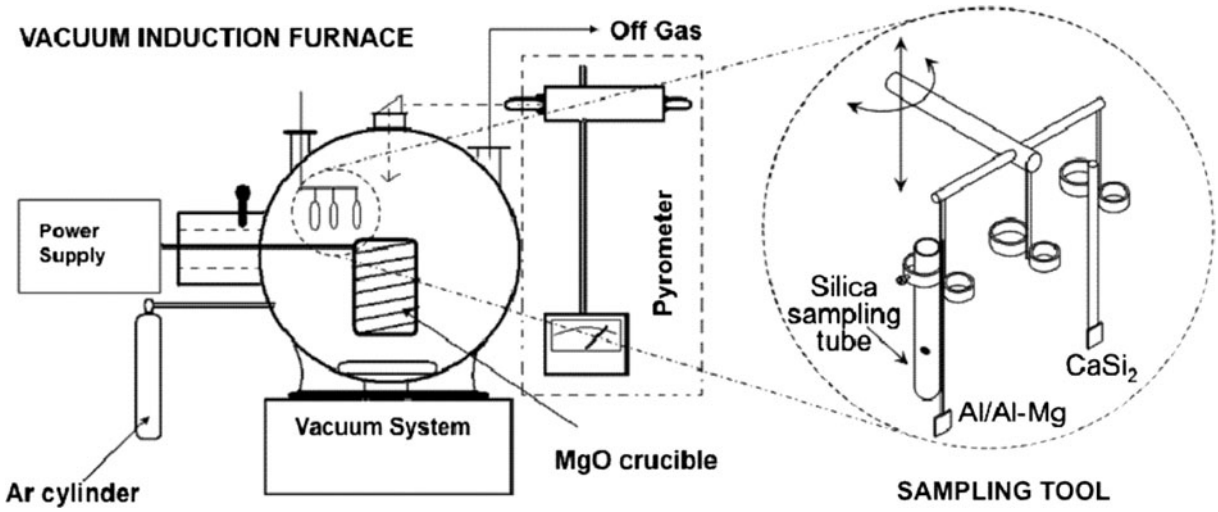

Fig. 2—Schematic of experimental setup and sampling tool.

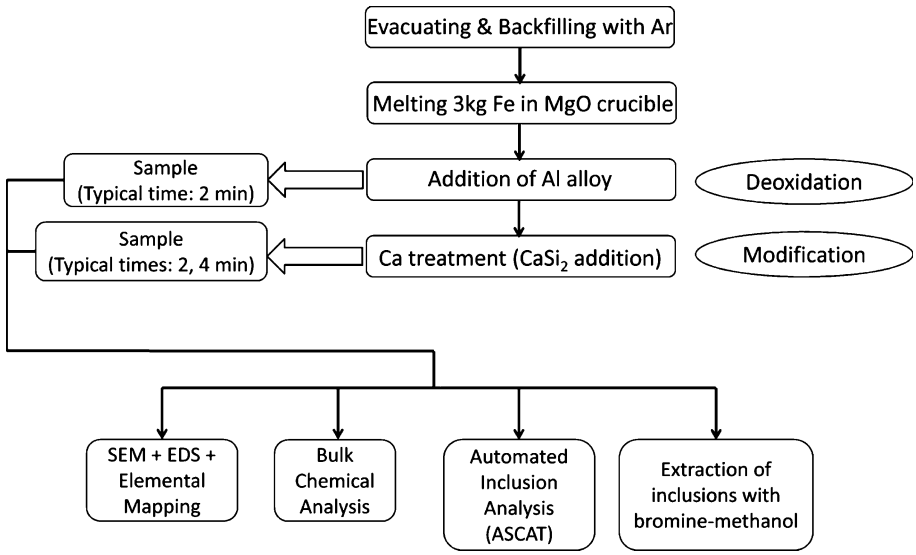

Fig. 3—Experimental procedure.

After all of the iron chips had melted (power input approximately 7.5 kW), the melt was held (at 1873 K [1600 °C]) for 20 minutes for homogenization. The aluminum shot (99.999 pct) was then added to the melt for deoxidation by lowering a steel sheet (2-mm-thick) capsule (containing the aluminum shot and attached to an iron wire of 2-mm diameter) into the melt. After lowering the capsule, the iron wire melted and the capsule dropped into the melt. Calcium treatment was subsequently performed by adding calcium silicide ($CaSi_2$) in powder form. The calcium silicide addition to molten steel is challenging as much of the calcium tends to vaporize because of its low boiling point. For the present experiments, calcium silicide powder was enclosed in a 4-mm-thick iron capsule attached to a 5-mm-diameter iron rod. The rod was used to submerge the capsule in the melt to make the calcium addition as deeply as possible. Liquid steel samples were taken after deoxidation (typically 2 minutes after the aluminum addition) and at various times (typically 2 minutes and 4 minutes) after calcium treatment. Because of the difficulties with calcium silicide additions, experiments were repeated or samples in different experiments were overlapped to test for reproducibility. Two sampling tube designs were used and compared, as is discussed subsequently.

D. *Characterization*

1. *Bulk chemical analysis*

Inductively coupled plasma spectroscopy was used to analyze Al, Mg, and Ca. The total oxygen content was measured by the inert gas fusion method (LECO N/O system, LECO Corporation, St. Joseph, MI), and the total sulfur content was measured with a carbon/sulfur analyzer (LECO C/S system).

2. *Inclusion microanalysis*

After samples were collected in sampling tubes, discs from the pin samples were machined and mounted in epoxy. SEM samples were prepared by wet grinding cross sections to 1200 grit followed by diamond polishing. Care was taken during manual polishing to avoid pulling inclusions out of the steel surface. Alumina or silica suspensions were avoided during polishing to minimize contamination.

3. *Automated inclusion microanalysis*

An automated steel cleanliness analysis tool (ASCAT) was used to determine the distribution of inclusion compositions; it is capable of analyzing hundreds of inclusions in a steel sample within minutes.[17] An ASCAT system consists of a SEM, an EDS analyzer, a digital scan generator under computer control, and control software. Most of the focusing and contrast/brightness threshold operations are automated. Inclusions are detected automatically based on back-scattered electron image contrast and analyzed automatically for size, composition, and morphology (instrument conditions: 20 keV, 220 × magnification, 18-mm working distance, and Si-drift detector at 45 deg elevation). Usually, inclusions larger than 1 μm in diameter were detected and analyzed. The threshold value for the detected elements (like Mg, Al, S, and Ca) was around 2 at. pct. ASCAT analysis of inclusions did not give any indication of the homogeneity of the inclusions. For this purpose, manual SEM analysis also was performed on selected inclusions (instrument conditions: 20 keV, 10-mm working distance, and Si-drift detector at 35 deg elevation).

4. *Extraction of inclusions by dissolution of the steel matrix*

Inclusions were extracted by dissolving steel samples (1 g) in a bromine-anhydrous methanol solution (100 mL volume, 10 pct bromine by mass) for 24 hours at room temperature.[18] This treatment dissolved the steel matrix, leaving the oxide inclusions behind; the inclusions were recovered by filtering the solution through a polycarbonate filter membrane with 0.2 μm openings (using an aspirator pump to create suction across the filter), subsequently rinsing the membrane with anhydrous methanol. After the methanol was evaporated, the membrane was mounted on a copper or brass stub (instead of the more commonly used aluminum stubs) and sputter coated with platinum (2 Å) for SEM. Sulfides were dissolved by the bromine-methanol solution,[18] but in steel samples that were subject to only partial dissolution (etching the steel surface), some inclusions containing sulfur could be observed at the steel surface.

E. *Quantifying the Effectiveness of Calcium Treatment*

The effectiveness of the calcium treatment was evaluated by the following two methods:

(a) Modified Ca/Al ratio[17]: Alumina inclusions are liquefied by reaction with calcium if a sufficiently high Ca:Al ratio is achieved in the oxide inclusion. However, it is necessary to correct for the contribution of CaS (often closely associated with oxide inclusion) to the calcium analysis. There is about 2 at. pct solubility of sulfur in the liquid calcium aluminate; assuming that the balance of the sulfur (pct S – 2 pct) is present as solid CaS, the molar ratio of Ca to Al in the modified inclusion (excluding CaS) was estimated as follows:

$$\left(\frac{\text{Ca}}{\text{Al}}\right)_{\text{mod}} = \frac{\text{pct Ca} - \text{pct S} + 2}{\text{pct Al}} \qquad [3]$$

where the compositions are in atomic percentages. Higher values of the modified Ca/Al ratio indicate higher degrees of modification of alumina inclusions by calcium.

(b) Distribution of inclusion compositions: ternary proportional symbol plots. In this work, the inclusions were compounds of calcium and aluminum with oxygen and sulfur. Because the valence of calcium and aluminum in the inclusions is fixed, inclusion compositions can be represented on ternary Al-Ca-S plots without losing any information about the oxygen content of the inclusions. To this end, inclusion compositions were normalized to 100 pct with respect to Al, Ca, and S.

To show the distribution of inclusion compositions, ternary proportional symbol plots were drawn, following the procedure illustrated in Figure 4. The procedure was to divide the ternary composition diagram into 400 congruent nonoverlapping triangles (with a 5 pct increment of one of the three components across the width of each triangle) and counting the number of inclusions with compositions in each triangle with a spreadsheet. To create the proportional symbol plot (using the statistical package R[19]), the inclusion count was used to scale each triangular symbol centered in the corresponding composition triangle. In the plot, the height of each symbol is proportional to the number of inclusions raised to the power n, where $n = 0.57$. (A value of $n = 0.5$ would cause the area of each symbol to be proportional to the number of inclusions, but because of the way in which areas are judged by human observers, $n = 0.57$ is preferred.[20]) The symbols were scaled such that the largest symbol had the same size in all plots and completely filled its composition triangle. Figure 4 illustrates the utility of this method, providing a clear indication of the distribution of inclusions; inclusion compositions plotting along the edges or at the corners of the composition triangles may be overlooked in the scatter plot but are clearly shown in the proportional symbol plot. Figure 4(a) shows the traditional Al-S-Ca ternary plot. Although these plots give a good indication of the change in inclusion compositions, a given point may represent a single inclusion or an unknown number of inclusions. This problem can be solved through the use of proportional symbol plots. For example, Figures 4(b) and (c) show that the specific sample contained a significant proportion of alumina (approximately 5 pct of all inclusions), which is not at all evident in the scatter plot (Figure 4(a)). In Figure 4(c), the dot–dash line gives the compositions that are 50 pct liquid at 1823 K (1550 °C) (as calculated with

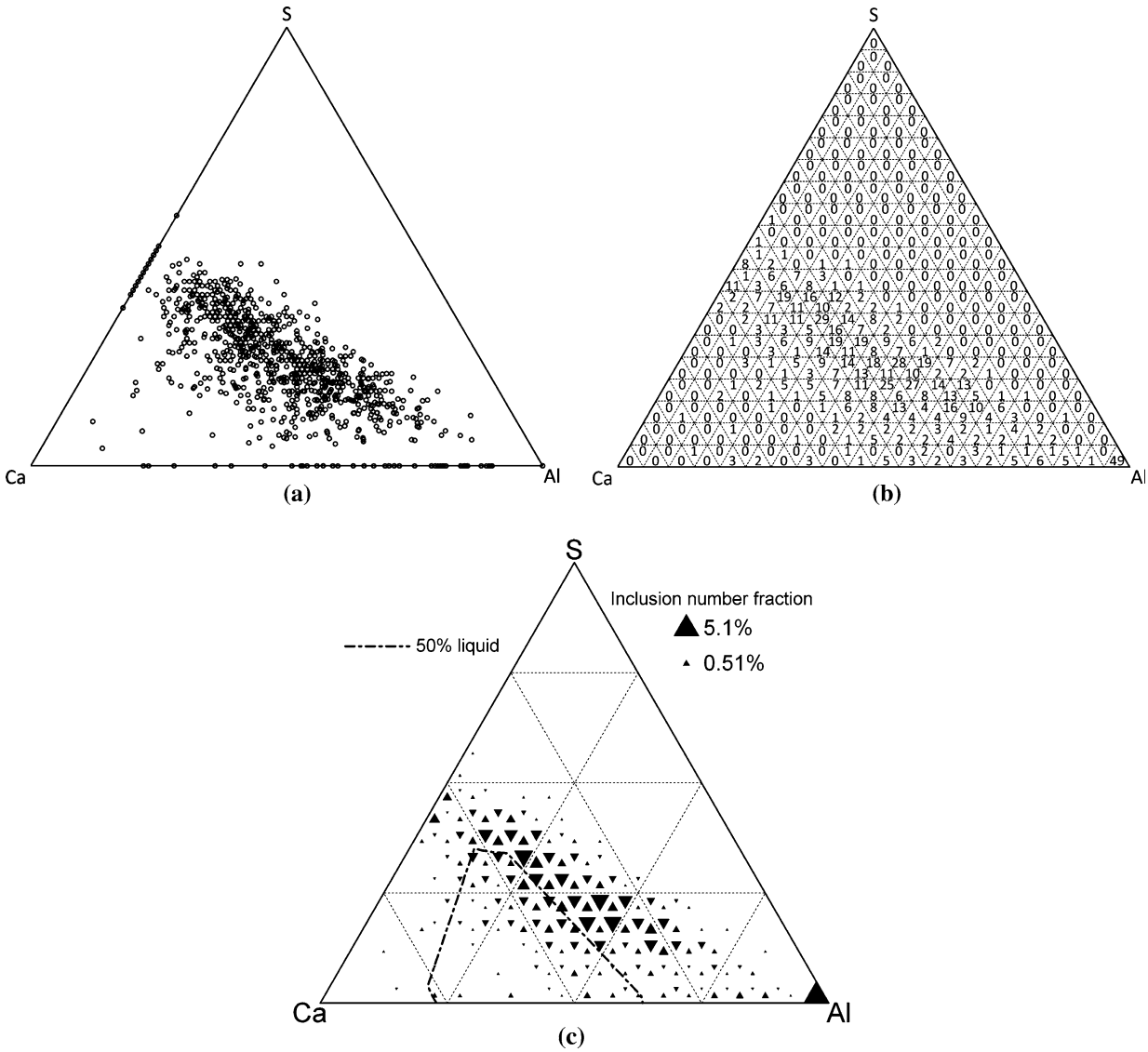

Fig. 4—Illustration of the procedure used to draw proportional symbol plots. (*a*) Scatter plot of analyses of 981 inclusions from a steel sample (plotted as mole fractions of Ca, S, and Al, excluding oxygen). (*b*) Numbers of inclusions with compositions in each of the 400 composition triangles. (*c*) Proportional symbol plot. The area of each triangle is proportional to the number of inclusions of which the compositions lie in that composition triangle.

FactSage 6.2, using the FSstel and FToxid database[7]); upon successful calcium modification, most inclusions would lie within this boundary. The definition used here is that the 50 pct liquid boundary represents phase compositions in which the liquid and solid contain an equal number of moles of cations (*i.e.*, the total number of moles of Ca and Al is the same in liquid and solid; S and O are not taken into account).

III. CHARACTERIZATION OF DEOXIDATION PRODUCTS AND THE EFFECT OF SAMPLER TYPE

A. *Aluminum Deoxidation Products*

Preliminary experiments were performed to determine the amount of Al required to reach 0.03 to 0.06 wt pct dissolved Al in the melt after deoxidation (similar to industrial melts); this was 3 g (for the 3 kg of laboratory melts). No oxygen was added to the iron; the oxygen present before deoxidation originated from the raw materials used in the experiment. Analysis of steel samples taken after deoxidation showed most inclusions to be pure alumina; however, occasionally, some Mg was detected in the inclusions (with the MgO crucible being the source). Figure 5 shows the irregular and agglomerated nature of these inclusions.

The experimental procedure included evacuating and backfilling the chamber with argon to avoid reoxidation. The effectiveness of this procedure was tested by sampling the steel melt 5 minutes, 10 minutes, and 20 minutes after deoxidation. The total aluminum content of the melt (mostly dissolved aluminum), remained essentially constant (Table I), whereas the inclusion content of the melt decreased consistently (Figure 6), as expected in the absence of reoxidation.

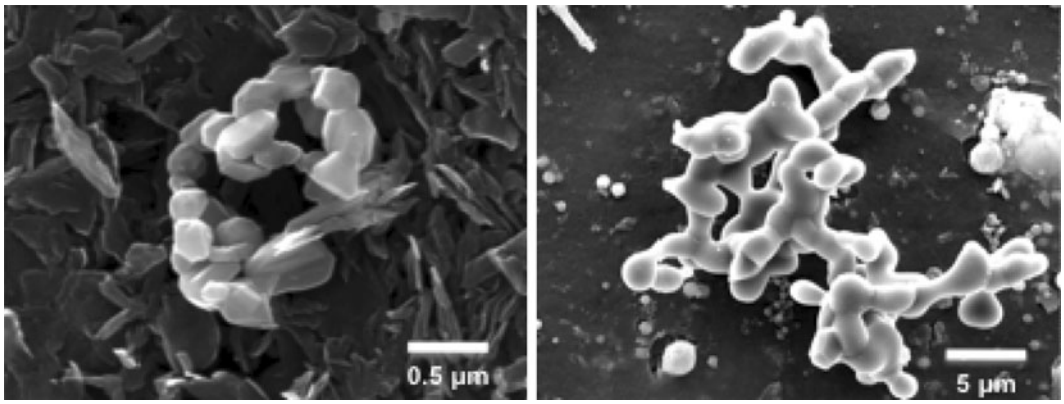

Fig. 5—Clustered alumina inclusions (extracted with bromine-methanol).

Table I. Total Aluminum Content in the Steel Samples Taken at Various Times After Aluminum Deoxidation (Accuracy of Chemical Analysis Results is ±0.002 pct)

Sample	Al (wt pct)
5 min after Al addition	0.060
10 min after Al addition	0.062
20 min after Al addition	0.054

With time, the size distribution shifted to smaller sizes (Figure 7) as larger inclusions preferentially floated out. In a separate test, the total oxygen content decreased sharply to 47 ppm in the first 2 minutes, reaching half this value after 30 minutes (Table II, Figure 8). This change between 2 minutes and 30 minutes is smaller than that suggested by the data in Figure 6; the probable reason for this is that the ASCAT results (used to draw Figure 6) exclude inclusions smaller than 1 μm, whereas the chemical analysis (used to determine the total oxygen content reported in Table II) does not. (The total oxygen is the sum of the dissolved oxygen, 3 to 4 ppm, and oxygen bound in inclusions. The large decrease in the total oxygen content from 450 ppm to around 50 ppm within 2 minutes indicates that the reaction between the aluminum and oxygen is fast, which is in agreement with Turkdogan's observations.[21]) Based on these observations, calcium modification was performed 2 minutes after aluminum deoxidation, in the laboratory heats.

Samples cut from a laboratory melt after solidification in the furnace (approximate size of ingot 3 kg, diameter 70 mm, and height 110 mm) similarly showed a much higher inclusion concentration at the top of the ingot, with much lower inclusion concentrations at the half height of the ingot both on the axis of the ingot and at the surface in contact with the crucible (Table III, Figure 9); the inclusions at the top surface were significantly larger (Figure 10).

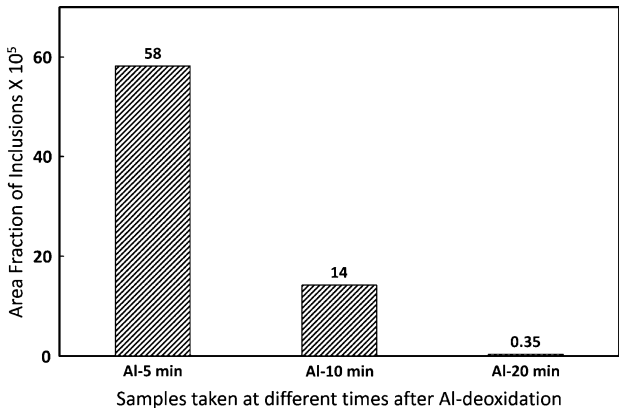

Fig. 6—Area fraction (measured by ASCAT) of alumina inclusions in steel samples taken at different times after aluminum deoxidation, showing progressive floating out of inclusions.

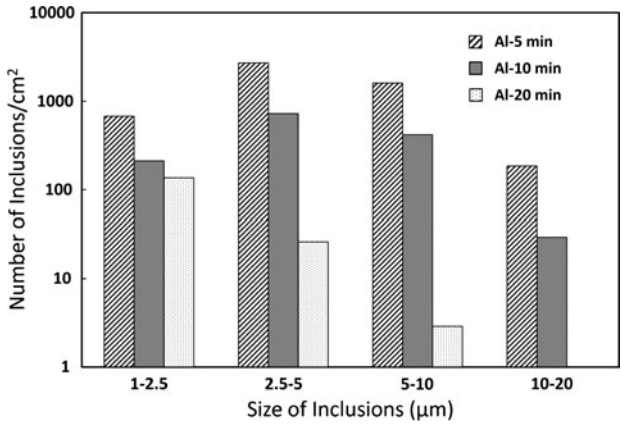

Fig. 7—Size distribution (measured by ASCAT) of inclusions in steel samples taken at various times after aluminum deoxidation.

B. *Effect of Sampler Type*

Given the uneven vertical distribution of inclusions in the melt, it was necessary to ensure that the samplers extracted samples that did not include the inclusions from the surface of the melt. The following types of fused-quartz samplers were compared:

(a) Sampler Type I: Gravity-fed, closed-end tube, with liquid steel entering through a hole on the side of the sampler (15-mm internal diameter, Figure 11)

Table II. Aluminum and Total Oxygen Content in Steel Samples Collected at Different Times After Aluminum Deoxidation

Sample	Al (wt pct)	Total Oxygen (ppm)
Before Al addition	0	450
2 min after Al addition	0.053	47
30 min after Al addition	0.050	23

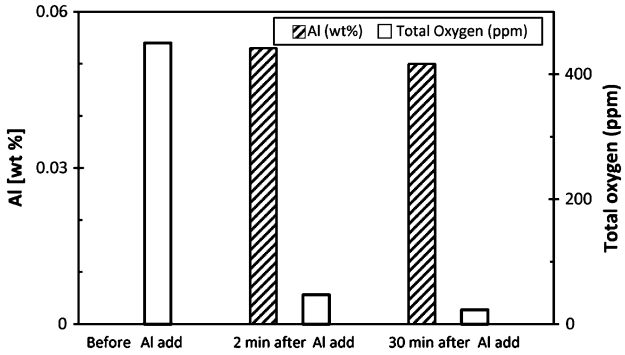

Fig. 8—Aluminum and total oxygen content in steel samples collected at different times after aluminum deoxidation. See Table II for values.

Table III. Inclusion Concentration and Area Fraction of Inclusions (ASCAT Measurements) at Different Positions in Solidified Experimental Melt

	Num/cm^2 of Inclusions	Area Fraction of Inclusions
Top sample	1.8×10^5	0.026
Center sample	110	9.4×10^{-6}
Side sample	102	9.5×10^{-6}

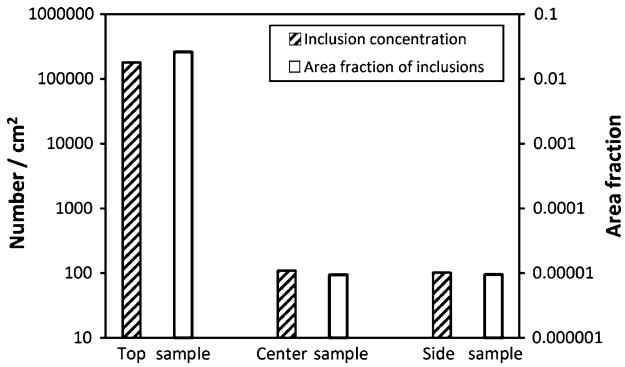

Fig. 9—Inclusion concentration and area fraction of inclusions (ASCAT measurements) at different positions in solidified experimental melt. See Table III for values.

(b) Sampler Type II: Vacuum sampler—an evacuated "pin" tube with a thinned end that ruptured within the melt (7-mm internal diameter)

Samples taken with the larger diameter sampler showed an apparent increase in inclusion concentration

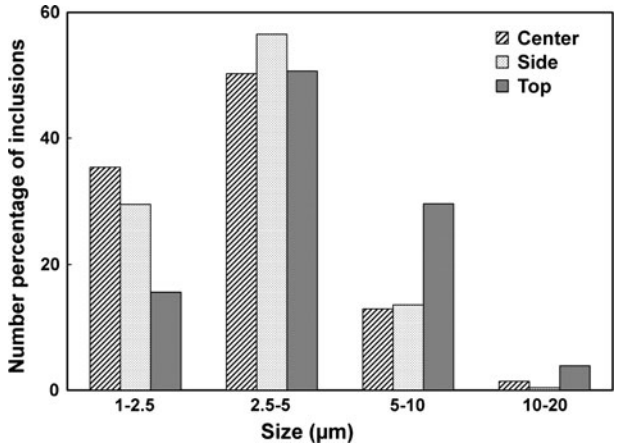

Fig. 10—Number percent size distribution of inclusions (measured by ASCAT) in samples from different positions in a solidified experimental ingot.

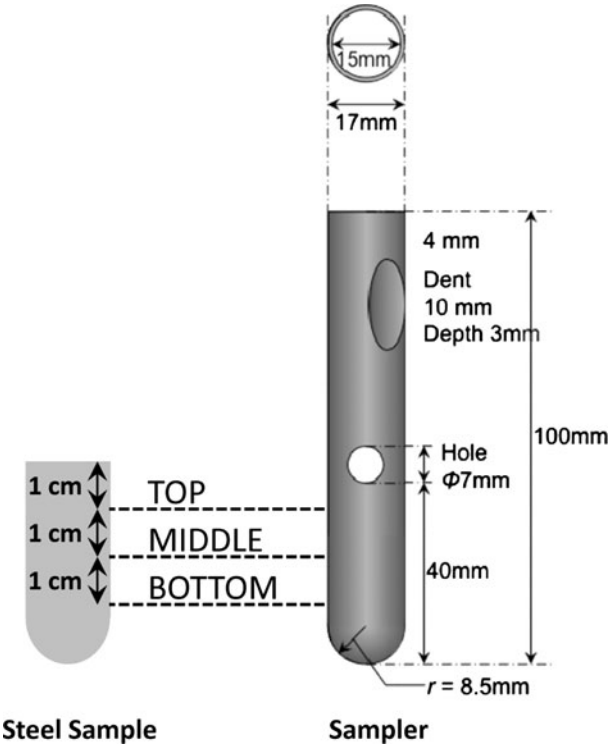

Fig. 11—Schematic of gravity-fed quartz sampler (type I), showing approximate positions of slices taken to measure inclusion distribution.

and total oxygen content after calcium treatment (Table IV); this result is not in agreement with the absence of reoxidation in the experiments. In separate experiments, the change in inclusion distribution with height in the sampler was measured (refer to Figure 11 for the positions of the examined cross sections). The results (Tables V and VI) show a significantly higher inclusion concentration at the top of the sample, suggesting flotation of the inclusions within the sampler before or during solidification. The much higher concentration of inclusions at the top of the sample taken

Table IV. Inclusion Area Fraction and Concentration (ASCAT Results) and Total Oxygen Content Before and After Calcium Treatment for Larger Diameter, Gravity-Fed Sampler (Type I) From Middle Part of the Sample

	Area Fraction (ppm)	Num/cm^2	Total Oxygen Content (ppm)
Before Ca treatment	12	269	10
After Ca treatment	130	1197	40

Table V. Inclusion Concentration and Area Fraction of Inclusions (ASCAT Results) in Slices at Various Heights in a Larger (Gravity-Fed) Sample Taken After Deoxidation

Position	Num/cm^2	Area Fraction (ppm)
Top	25,458	1560
Middle	1068	43
Bottom	1041	48

Table VI. Inclusion Concentration and Area Fraction of Inclusions (ASCAT Results) in Slices at Various Heights in a Larger (Gravity-Fed) Sample Taken After Calcium Treatment (Same Heat as Table V)

Position	Num/cm^2	Area Fraction (ppm)
Top	4825	233
Middle	3428	67
Bottom	2982	57

Table VII. Area Fraction of Inclusions and Inclusion Concentration (ASCAT Results) for Different Sampler Types (Larger Diameter, Gravity-Fed, and Smaller Diameter, Vacuum Samplers) Before and After Ca Treatment

Sample	Sampler	Area Fraction (ppm)	Num/cm^2
Before Ca treatment	Type I (larger diameter)	50	2195
	Type II (smaller diameter)	160	4138
After Ca treatment	Type I (larger diameter)	110	6121
	Type II (smaller diameter)	80	8718

before calcium treatment is in line with the observation (discussed in the second section) that the inclusion size decreased after calcium treatment; the larger alumina (deoxidation product) inclusions have a greater tendency to float out, and hence, the central part of the sample is depleted of inclusions.

The smaller-diameter vacuum samplers largely avoided the negative effects of differential flotation of larger and smaller inclusions, as demonstrated in trials in which both sampler types were used on the same laboratory heat. Table VII shows the area fractions and inclusion concentrations of samples collected before and after calcium treatment using both sampler types.

Of the samples collected before calcium treatment (larger inclusions), the smaller diameter vacuum samplers yielded a significantly larger inclusion count and area fraction than the larger, gravity-fed samplers. Taking samples with the larger diameter samplers seems to result in undercounting of inclusions, presumably because inclusions floated out during solidification in the sampler. The sample collected after Ca treatment did not show a significant difference in area fraction and inclusion concentration between the vacuum sampler and quartz tube, which is in line with the smaller inclusion size after calcium treatment. Hence, the vacuum samplers were preferred both because these took samples from deeper within the melt (and hence were more representative of the bulk of the steel) and because their smaller internal diameter would cause the sample to solidify more rapidly with less flotation of inclusions within the sampler.

IV. SUMMARY AND CONCLUSIONS

This first part of this study describes the methodology adopted to study the transient behavior of inclusions upon calcium treatment of alumina inclusion. Automated inclusion analysis (ASCAT) was used to obtain the distribution of inclusion compositions; the distributions were plotted as proportional symbol diagrams. Inclusion flotation occurred both within the experimental melt and in liquid steel samples taken from the melt. Smaller diameter vacuum samplers were more representative of the melt as they were sampled from deeper in the melt and produced more rapid sample solidification than in the larger diameter, gravity-fed samples.

The second section presents results of modification of alumina inclusions by calcium (based on laboratory and industrial samples), illustrating the formation of transient (nonequilibrium) reaction products upon calcium treatment and presenting a proposed reaction mechanism for the modification of alumina inclusions by calcium at different sulfur contents in the steel.

ACKNOWLEDGMENTS

Support for this work by the industrial members of the Center for Iron and Steelmaking Research is gratefully acknowledged.

REFERENCES

1. A.W. Cramb: in *Impurities in Engineering Materials*, C.L. Briant, ed., Marcel Dekker, New York, NY, 1999, pp. 49–89.
2. G.J.W. Kor: *Proc. First Int. Calcium Treatment Symp*, The Institute of Metals, London, U.K., 1988, pp. 39–44.
3. N. Verma, M. Lind, P.C. Pistorius, R.J. Fruehan, and M. Potter: *Iron Steel Tech.*, 2010, vol. 7 (7), pp. 189–97.
4. G.M. Faulring, J.W. Farrell, and D.C. Hilty: *Iron Steelmaker*, 1980, vol. 7 (2), pp. 14–20.
5. B. Deo and R. Boom: *Fundamentals of Steelmaking Metallurgy*, Prentice Hall International, Hemel Hempstead, U.K., 1993, pp. 265–69.

6. G.J.W. Kor: *The Elliott Symposium*, Iron and Steel Society, Warrendale, PA, 1990, pp. 400–17.
7. C.W. Bale, P. Chartrand, S.A. Degterov, G. Eriksson, K. Hack, R. Ben Mahfoud, J. Melançon, A.D. Pelton, and S. Petersen: *CALPHAD*, 2002, vol. 26, pp. 189–228.
8. G.K. Sigworth and J.F. Elliott: *Met. Sci.*, 1974, vol. 8, pp. 298–310.
9. D. Lu, G.A. Irons, and W.K. Lu: *Proc. First Int. Calcium Treatment Symp*, The Institute of Metals, London, U.K., 1988, pp. 23–30.
10. Y. Higuchi, M. Numata, S. Fukagawa, and K. Shinme: *ISIJ Int.*, 1996, vol. 36, pp. S151–S154.
11. W. Tiekink, B. Santillana, R. Boom, R. Kooter, F. Mensonides, and B. Deo: *Iron Steel Tech.*, 2008, vol. 5 (9), pp. 185–95.
12. J.C. Anglezio, C. Servant, and I. Ansara: *CALPHAD*, 1994, vol. 18, pp. 273–309.
13. I.-H. Jung, S.A. Decterov, and A.D. Pelton: *Metall. Mater. Trans. B*, 2004, vol. 35B, pp. 493–507.
14. J.M.A. Geldenhuis and P.C. Pistorius: *Ironmaking Steelmaking*, 2000, vol. 27, pp. 442–49.
15. Y. Wang, M. Valdez, and S. Sridhar: *Metall. Mater. Trans. B*, 2002, vol. 33B, pp. 625–32.
16. H. Matsuura, C. Wang, G. Wen, and S. Sridhar: *ISIJ Int.*, 2007, vol. 48, pp. 1265–74.
17. S.R. Story, T. Piccone, R.J. Fruehan, and M. Potter: *Iron Steel Tech.*, 2004, vol. 1 (9), pp. 163–69.
18. T.R. Dulski: *A Manual for the Chemical Analysis of Metals*, American Society for Testing and Materials, West Conshohocken, PA, 1996, pp. 89–90.
19. R Development Core Team: R: *A Language and Environment for Statistical Computing, R Foundation for Statistical Computing*, Vienna, Austria, 2010, http://www.R-project.org/.
20. J.J. Flannery: *Canadian Cartographer*, 1971, vol. 8, pp. 96–109.
21. E.T. Turkdogan: *Arch. Eisenhuettenwes.*, 1983, vol. 54, pp. 1–10.